Incomplete Retinal Pigment Epithelial and Outer Retinal Atrophy (iRORA) in Age-related Macular Degeneration: CAM Report 4

Article *in* Ophthalmology · September 2019

DOI: 10.1016/j.ophtha.2019.09.035

CITATIONS
91

READS
1,719

30 authors, including:

Philip J Rosenfeld
University of Miami Miller School of Medicine
278 PUBLICATIONS **23,659** CITATIONS
SEE PROFILE

Christine A Curcio
University of Alabama at Birmingham
316 PUBLICATIONS **24,112** CITATIONS
SEE PROFILE

Frank Gerhard Holz
University of Bonn
876 PUBLICATIONS **26,138** CITATIONS
SEE PROFILE

Giovanni Staurenghi
University of Milan
308 PUBLICATIONS **10,374** CITATIONS
SEE PROFILE

AMERICAN ACADEMY OF OPHTHALMOLOGY®

Incomplete Retinal Pigment Epithelial and Outer Retinal Atrophy in Age-Related Macular Degeneration

Classification of Atrophy Meeting Report 4

Robyn H. Guymer, MBBS, PhD,[1] Philip J. Rosenfeld, MD, PhD,[2] Christine A. Curcio, PhD,[3] Frank G. Holz, MD,[4] Giovanni Staurenghi, MD,[5] K. Bailey Freund, MD,[6] Steffen Schmitz-Valckenberg, MD,[4] Janet Sparrow, PhD,[7] Richard F. Spaide, MD,[6] Adnan Tufail, MD,[8] Usha Chakravarthy, MD, PhD,[9] Glenn J. Jaffe, MD,[10] Karl Csaky, MD,[11] David Sarraf, MD,[12] Jordi M. Monés, MD, PhD,[13] Ramin Tadayoni, MD, PhD,[14] Juan Grunwald, MD,[15] Ferdinando Bottoni, MD,[5] Sandra Liakopoulos, MD,[16] Daniel Pauleikhoff, MD,[17] Sergio Pagliarini, MD,[18] Emily Y. Chew, MD,[19] Francesco Viola, MD,[20] Monika Fleckenstein, MD,[4] Barbara A. Blodi, MD,[21] Tock Han Lim, MD,[22] Victor Chong, MD, PhD,[23] Jerry Lutty, PhD,[24] Alan C. Bird, MD,[8] Srinivas R. Sadda, MD[25]

Purpose: To describe the defining features of incomplete retinal pigment epithelium (RPE) and outer retinal atrophy (iRORA), a consensus term referring to the OCT-based anatomic changes often identified before the development of complete RPE and outer retinal atrophy (cRORA) in age-related macular degeneration (AMD). We provide descriptive OCT and histologic examples of disease progression.

Design: Consensus meeting.

Participants: Panel of retina specialists, including retinal imaging experts, reading center leaders, and retinal histologists.

Methods: As part of the Classification of Atrophy Meeting (CAM) program, an international group of experts analyzed and discussed longitudinal multimodal imaging of eyes with AMD. Consensus was reached on a classification system for OCT-based structural alterations that occurred before the development of atrophy secondary to AMD. New terms of iRORA and cRORA were defined. This report describes in detail the CAM consensus on iRORA.

Main Outcome Measures: Defining the term *iRORA* through OCT imaging and longitudinal cases showing progression of atrophy, with histologic correlates.

Results: OCT was used in cases of early and intermediate AMD as the base imaging method to identify cases of iRORA. In the context of drusen, iRORA is defined on OCT as (1) a region of signal hypertransmission into the choroid, (2) a corresponding zone of attenuation or disruption of the RPE, and (3) evidence of overlying photoreceptor degeneration. The term *iRORA* should not be used when there is an RPE tear. Longitudinal studies confirmed the concept of progression from iRORA to cRORA.

Conclusions: An international consensus classification for OCT-defined anatomic features of iRORA are described and examples of longitudinal progression to cRORA are provided. The ability to identify these OCT changes reproducibly is essential to understand better the natural history of the disease, to identify high-risk signs of progression, and to study early interventions. Longitudinal data are required to quantify the implied risk of vision loss associated with these terms. The CAM classification provides initial definitions to enable these future endeavors, acknowledging that the classification will be refined as new data are generated. *Ophthalmology 2020;127:394-409 © 2019 by the American Academy of Ophthalmology*

Supplemental material available at www.aaojournal.org.

Geographic atrophy (GA) is a late-stage disease manifestation in nonneovascular age-related macular degeneration (AMD) that progresses to severe central vision loss. Geographic atrophy has traditionally been defined on color fundus photography (CFP) as a sharply delineated circular or oval area of hypopigmentation or depigmentation in which choroidal vessels are visible. The size requirement for GA varies with the different studies, ranging from one eighth to one fourth of a disc area (corresponding roughly to 175 μm and 430 μm in diameter, respectively) on CFP.[1,2]

https://doi.org/10.1016/j.ophtha.2019.09.035
ISSN 0161-6420/19

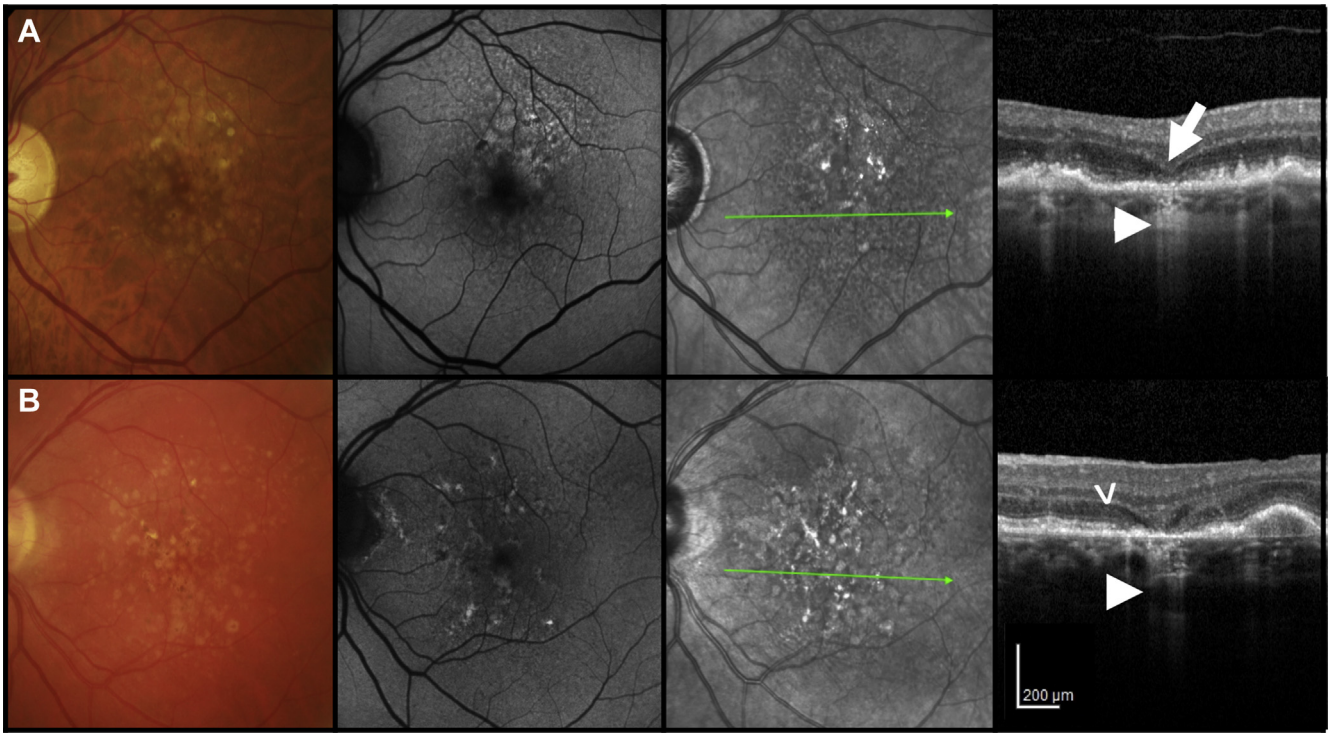

Figure 1. Examples of multimodal imaging features of incomplete retinal pigment epithelium and outer retinal atrophy (iRORA); color fundus photography (CFP; first column), fundus autofluorescence (FAF; second column), near-infrared reflectance (NIR; third column), and OCT B-scan (fourth column). **A**, **B**, Left maculae of 2 individual cases with large drusen. The first column shows CFP demonstrating drusen and pigmentary changes without evidence of geographic atrophy. The second column shows FAF imaging demonstrating only small areas of hypoautofluorescence. The third column shows NIR images illustrating no evidence of atrophy. The fourth column shows OCT B-scans demonstrating subsidence of the inner nuclear layer (large arrow) and outer plexiform layer. Note the hyporeflective wedge-shaped band within the limits of the Henle fibre layer (**B,** arrowhead). Note the loss of photoreceptors as evidenced by outer nuclear layer thinning and loss of external limiting membrane, ellipsoid zone, and interdigitation zone. Subjacent to the area of photoreceptor loss is a zone of attenuation and disruption of the retinal pigment epithelium (<250 µm). A region of signal hypertransmission into the choroid is less than 250 µm in continuity (small arrow). This fulfills the criteria for iRORA.

Geographic atrophy was retained as a term for a late stage of AMD in the 2013 Beckman CFP classification of AMD.[3]

As a clinical trial end point, the ability to slow GA expansion using a novel therapy has been approved by regulatory authorities, in which atrophy can be defined and quantified by fundus autofluorescence (FAF).[4–6] Recent trials aiming to slow progression of atrophy were required to enroll eyes with established regions of GA that could be measured reliably by a reading center, usually measuring at least 0.5 to 1.0 disc areas (1.25–2.5 mm^2).[7–9] It is preferable to initiate treatment earlier in the disease process, before GA is detectable. However, this strategy requires a clinical trial end point focused on the prevention of GA onset, rather than the progression of preexisting GA lesions.[10]

Previous studies have identified characteristic fundus features that are associated with a high risk for progression to GA. The Age-Related Eye Disease Study determined that large drusen within the central macula and pigmentary changes identified on CFP confer risk.[11] More recently, multimodal imaging, including OCT, has identified other macular features that increase the risk of vision loss, including increased drusen volume, decreased internal reflectivity of drusen (identified as calcified drusen), intraretinal hyperreflective foci, and subretinal drusenoid deposits (also known as reticular pseudodrusen).[12–22] In addition, as drusen regress, the overlying retinal layers undergo characteristic changes in progressing to atrophy that can be captured on OCT imaging. These changes, referred to as nascent GA (nGA) in previous reports, include subsidence of the inner nuclear layer (INL) and outer plexiform layer (OPL), a hyporeflective wedge-shaped band within the Henle fiber layer (HFL), often accompanied by RPE disturbance, and increased signal hypertransmission into the choroid.[23–26] With the recent advances in OCT angiography, more is being learned about other potential biomarkers of progression risk.[27,28] Therefore, when clinical trials are being designed for agents that aim to prevent atrophy development, it will be important to take these clinical variables into account. Using these variables will make it possible to enroll eyes at high risk and thus likely to progress to atrophy within a clinically relevant timeframe.

To characterize further the anatomic biomarkers that predict GA development, experts of the Classification of Atrophy Meeting (CAM) group addressed this topic. This group was convened to explore the use of multimodal imaging and to devise a new consensus nomenclature for the different stages of AMD, as well as to explore new strategies to identify and determine our ability to capture early stages reproducibly using OCT. To determine stages of disease

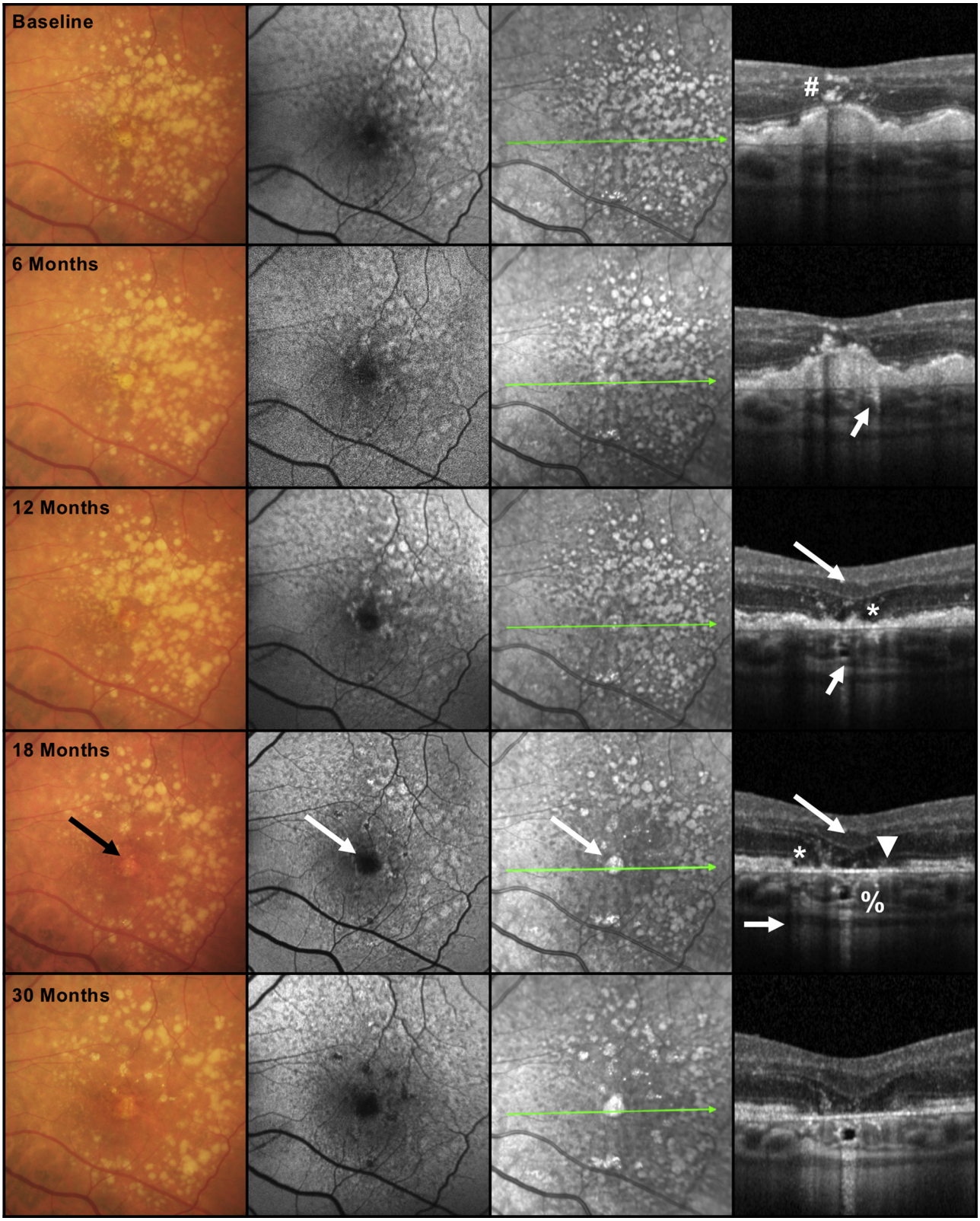

Figure 2. Multimodal imaging of an age-related macular degeneration case illustrating progression from incomplete retinal pigment epithelium (RPE) and outer retinal atrophy (iRORA) to complete RPE and outer retinal atrophy (cRORA) over 30 months: color fundus photography (CFP; first column), fundus autofluorescence (FAF; second column), near infrared reflectance (NIR; third column), and OCT B-scan fourth (column). The images are CFP of the left macula in a case with large drusen and hyperpigmentation, reticular pseudodrusen on FAF, and hyperreflective foci (number sign) on OCT at baseline.

progression, case examples with longitudinal follow-up were provided and studied by the group.

In the first 2 CAM reports, the definition of the term *GA* in the ophthalmologic literature was reviewed, and guidelines for the application of various imaging methods for clinical research in AMD were generated.[29,30] In the third CAM report, OCT was recommended as the base or reference method to identify early atrophic changes, with other methods used for confirmation. The CAM group also recommended that the atrophic stages of AMD should be named according to the affected anatomic layers on OCT.[31] In that report, the term *complete RPE and outer retinal atrophy* (cRORA) was proposed as an end point for atrophy that occurred in the presence of drusen and was defined by the following criteria: (1) a region of hypertransmission of at least 250 μm in diameter, (2) a zone of attenuation or disruption of the RPE of at least 250 μm in diameter, and (3) evidence of overlying photoreceptor degeneration, all occurring in the absence of signs of an RPE tear.[31] The term *incomplete RPE and outer retinal atrophy* (iRORA) was introduced to describe a stage of AMD in which these OCT signs were present but did not fulfill all the criteria for cRORA.

In this report, we describe in detail the necessary OCT features that define iRORA and demonstrate longitudinal progression from this earlier stage to cRORA with illustrated case examples and histologic correlates. We also provide corresponding images from other methods as they play a role in validating that the atrophic process has commenced. These case examples are intended to allow the AMD clinical and research community, as well as industry and regulatory bodies, to become familiar with the advances made in understanding the progression from drusen to GA in AMD and the proposed OCT nomenclature that is critical for ensuring harmonization when describing these changes. Progression sequences to atrophy from precursor signs other than drusen (e.g., subretinal drusenoid deposits) do occur, and these will be addressed in a separate report.

Methods

Classification of Atrophy Meeting Group

An international team of experts in AMD, retinal imaging, and histopathology was assembled to develop multimodal definitions of atrophy in the setting of AMD. The selection of members has been described elsewhere and included clinician scientists, experts in retinal imaging, image reading center leaders, clinical trialists, and histologists (the full list of participants is provided in Appendix 1, available at www.aaojournal.org).[31] Representatives from pharmaceutical and imaging device companies attended the meetings as observers.

Classification of Atrophy Meeting Group Meetings and Overview of Consensus Methodology

The CAM Group met on 5 occasions: June 2015, September 2015, June 2016, February 2018, and January 2019. Classification of Atrophy Meeting participants contributed longitudinal case studies that displayed the various OCT features of atrophy to stimulate open discussion and analysis at each meeting. The pathway to consensus has been outlined elsewhere.[31] In brief, participants were asked to review image sets and to identify anatomic features in atrophic areas and in the junctional zone between normal retina at the margins of atrophy. In longitudinal cases, CAM participants were asked to determine the time point at which atrophy was first noted, using each of several imaging methods independently, including CFP, near infrared reflectance, FAF, and OCT (cross-sectional and en face). The definitions described in the CAM report 3 and in this report are intended to be applied in the setting of AMD, a disease currently defined by the presence of drusen with or without subretinal drusenoid deposits. For this report, multimodal imaging of cases that best demonstrated signs of iRORA and progression to cRORA are highlighted. In addition, cases without the full complement of iRORA signs are shown to depict variation in presentation before the development of cRORA.

Results

Incomplete Retinal Pigment Epithelium and Outer Retinal Atrophy

The CAM 3 meeting established that nomenclature for the pathologic process that could be observed as the disease progressed toward GA would be based on the specific retinal layers affected (Fig 1). In the context of AMD with conventional drusen, iRORA is defined on OCT by the following criteria: (1) a region of signal hypertransmission into the choroid, (2) a corresponding zone of attenuation or disruption of the RPE, with or without persistence of basal laminar deposits, and (3) evidence of overlying photoreceptor degeneration, that is, subsidence of the INL and OPL, presence of a hyporeflective wedge in the HFL, thinning of the outer nuclear layer (ONL), disruption of the external limiting membrane (ELM), or disintegrity of the ellipsoid zone (EZ), and when these criteria do not

Disruption of some outer retinal bands and the RPE are present, but no definite hypertransmission is present, so the criteria for iRORA are not met. At 6 months, hypertransmission into the choroid is seen on OCT (small arrow), so iRORA criteria are now met. At 12 months, iRORA is more definitely seen on the OCT with RPE disruption less than 250-μm wide (asterisk), with remaining RPE cells difficult to distinguish from persistent basal laminar deposits (BLamDs). Subsidence of the inner nuclear layer (INL), outer plexiform (OPL), an external limiting membrane (ELM) descent are present on either side of the atrophy (large arrow), with corresponding hypertransmission (small arrow). No definite evidence is visible of GA on CFP or atrophy on either FAF or NIR. At 18 months, the eye progressed to cRORA or GA on CFP (black arrow) and to atrophy on FAF and NIR (white arrow). The OCT illustrates evidence of photoreceptor loss: subsidence of the INL and OPL, thinning of the ONL, discontinuous ELM descending on the sides of the atrophy, discontinuity of the ellipsoid zone and interdigitation zone (large arrow), an area of complete RPE disruption (without residual BLamD) of more than 250 μm (asterisk) showing a bare Bruch's membrane (arrowhead), and increased hypertransmission of more than 250 μm (small arrow). At 30 months, the initial atrophic area has changed little compared with that at 18 months, but additional areas of atrophy are becoming apparent on FAF and NIR. The hyporeflective space in the choroid at 18 and 30 months has been described as a choroidal cavern (%).

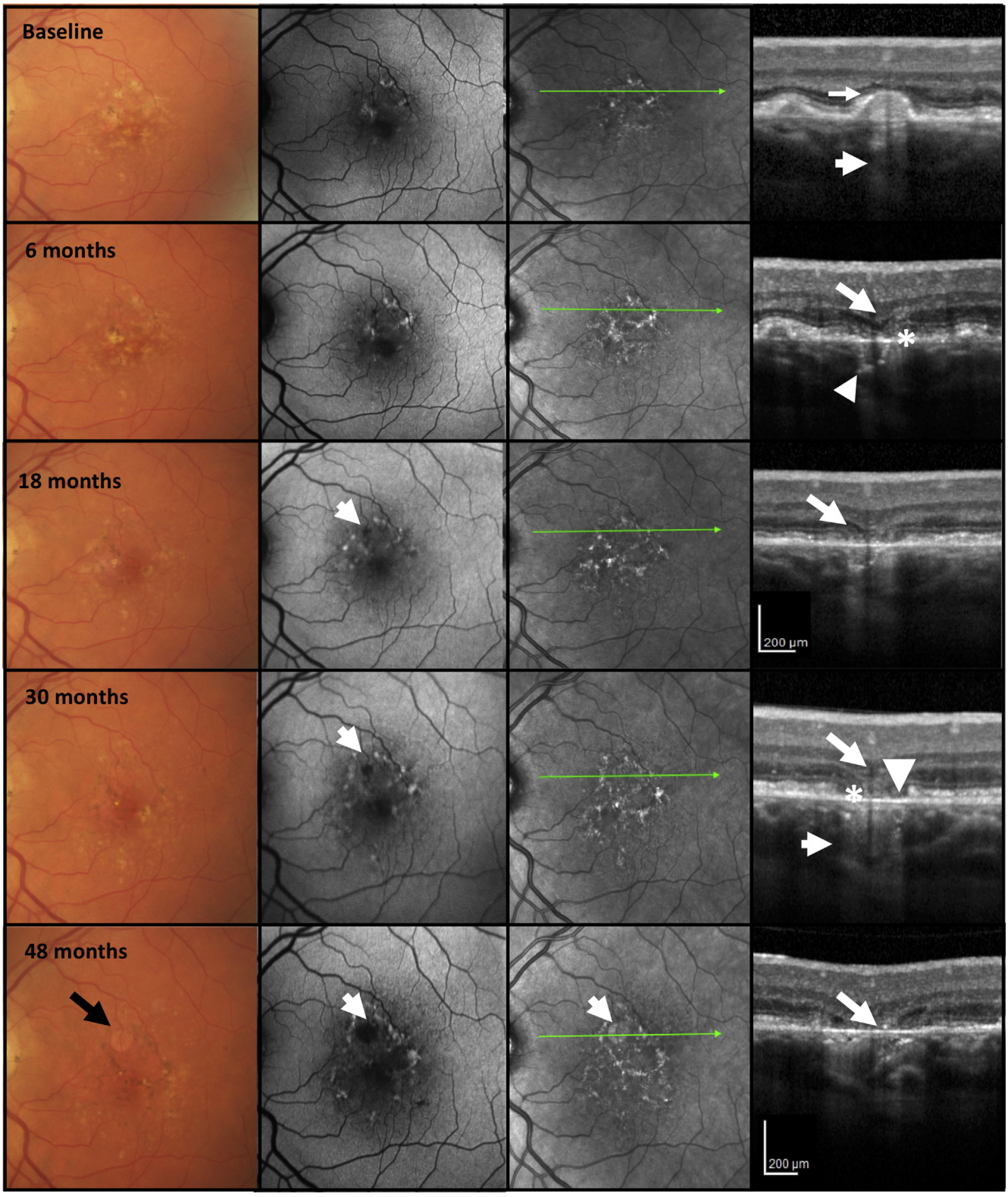

Figure 3. Multimodal imaging of an age-related macular degeneration case illustrating progression from incomplete retinal pigment epithelium (RPE) and outer retinal atrophy (iRORA) to complete RPE and outer retinal atrophy (cRORA) over 48 months: color fundus photography (CFP; first column), fundus autofluorescence (FAF; second column), near-infrared reflectance (NIR; third column), and OCT B-scan (fourth column). Color fundus photography of the left macula illustrates large drusen and hyperpigmentation at baseline. Fundus autofluorescence shows areas of hypoautofluorescence and hyperautofluorescence. The OCT at baseline shows a large druse, demonstrating hypertransmission into the choroid (small arrow). The external limiting

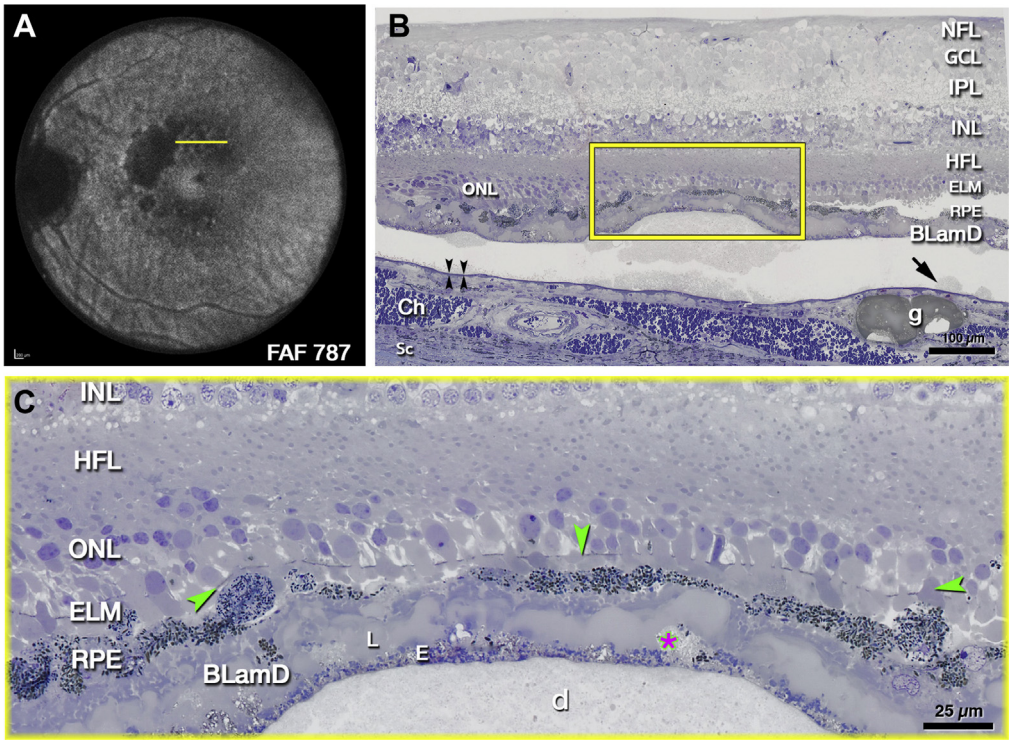

Figure 4. Images showing the external limiting membrane (ELM) approaching the druse apex because of photoreceptor shortening. The histologic evidence supports the clinical imaging in Figures 2 and 3 and illustrates changes in photoreceptor layers above a large druse as the atrophic process begins. **A**, Ex vivo imaging of the left eye of an 85-year-old white female donor with geographic atrophy. Areas of absent autofluorescence signal (787 nm) indicate complete retinal pigment epithelium (RPE) and outer retinal atrophy (cRORA). Yellow line crosses an area of mottled autofluorescence shown on histologic analysis. **B**, **C**, Submicrometer epoxy sections of osmium tannic acid paraphenylenediamine postfixed tissue stained with toluidine blue, at the plane indicated in (**A**). **B**, Retina, RPE, and basal laminar deposit (BLamD) are artifactually detached from Bruch's membrane (black arrowheads) at a soft druse and surrounding basal linear deposit (arrow). **C**, Framed area is magnified. Intact ELM (green arrowheads) skims close to the druse (d) apex, because photoreceptor outer segments are absent and inner segments are markedly shortened. Retinal pigment epithelium atop the druse is dysmorphic or absent. Basal laminar deposits (BLamDs) are thick with sublayers, including basal mounds (asterisk). Ch = choroid; E = early Henle fiber layer; g = Friedman lipid globule; GCL = ganglion cell layer; HFL = Henle fiber layer; IPL = inner plexiform layer; L = late Henle fiber layer; NFL = nerve fiber layer; ONL = outer nuclear layer; Sc = sclera. Histologic analysis and figure prepared by J. D. Messinger, DC, from the Project MACULA resource (http://projectmacula.cis.uab.edu/).

meet the definition of cRORA. The term *iRORA* should not be used in the presence of an RPE tear. Corroborating signs on CFP, FAF, and near-infrared reflectance are not required because they are not always evident (Fig 1).

Progression of Incomplete Retinal Pigment Epithelium and Outer Retinal Atrophy

Review of longitudinal follow-up of many cases (50 longitudinal cases were reviewed formally and were assessed by all CAM members, then collected and analyzed before CAM meetings, with these results presented and discussed as well as many other cases presented during the meetings) with iRORA confirms that these areas progress and develop into cRORA over a variable period ranging from months to years.

Examples of progression in 2 cases, imaged every 6 months, are illustrated in Figures 2 and 3. In both cases, baseline B-scans reveal eyes with large drusen, in which the ELM appears to be disrupted over the apex of a druse. The

membrane (ELM) is not seen clearly on top of this druse (large arrow), and the RPE appears intact. As such, the criteria for iRORA are not present. At 6 months, little change is evident in CFP, FAF, and NIR, but on OCT, iRORA has developed, with subsidence of the inner nuclear (INL) and outer plexiform (OPL) layers (large arrow), thinning of the outer nuclear layer (ONL), and subsidence of the ELM, which remains continuous. The ellipsoid zone (EZ) and RPE are discontinuous (asterisk), and increased hypertransmission into the choroid is present (small arrow). At 18 months, although little change is present on the CFP, now a hypoautofluorescent area is apparent on FAF (small arrow). On OCT, a definite descent and disruption of the ELM on either side of the atrophic area are evident, and in the midst of the atrophic area, OPL and INL subsidence (large arrow), further disruption of RPE, and possible basal laminar deposits remain on Bruch's membrane (BrM). At 30 months, cRORA and atrophy on the FAF are evident, whereas CFP does not demonstrate geographic atrophy (GA). OCT harbors evidence of photoreceptor loss; subsidence of the INL and OPL, thinning of the ONL, discontinuous ELM descending on both sides of the atrophic area, discontinuity of the EZ and interdigitation zone (IZ; large arrow), an area of complete RPE disruption (asterisk) without residual BLamD of more than 250 µm in width and showing a bare BrM (arrowhead), and hypertransmission of more than 250 µm (small arrow). At 48 months, GA is identified on CFP (black arrow), an enlarged area of atrophy on FAF is apparent, and atrophy is noted on the NIR image (white arrow). On OCT, the subsiding OPL within the atrophic area approaches BrM (large arrow).

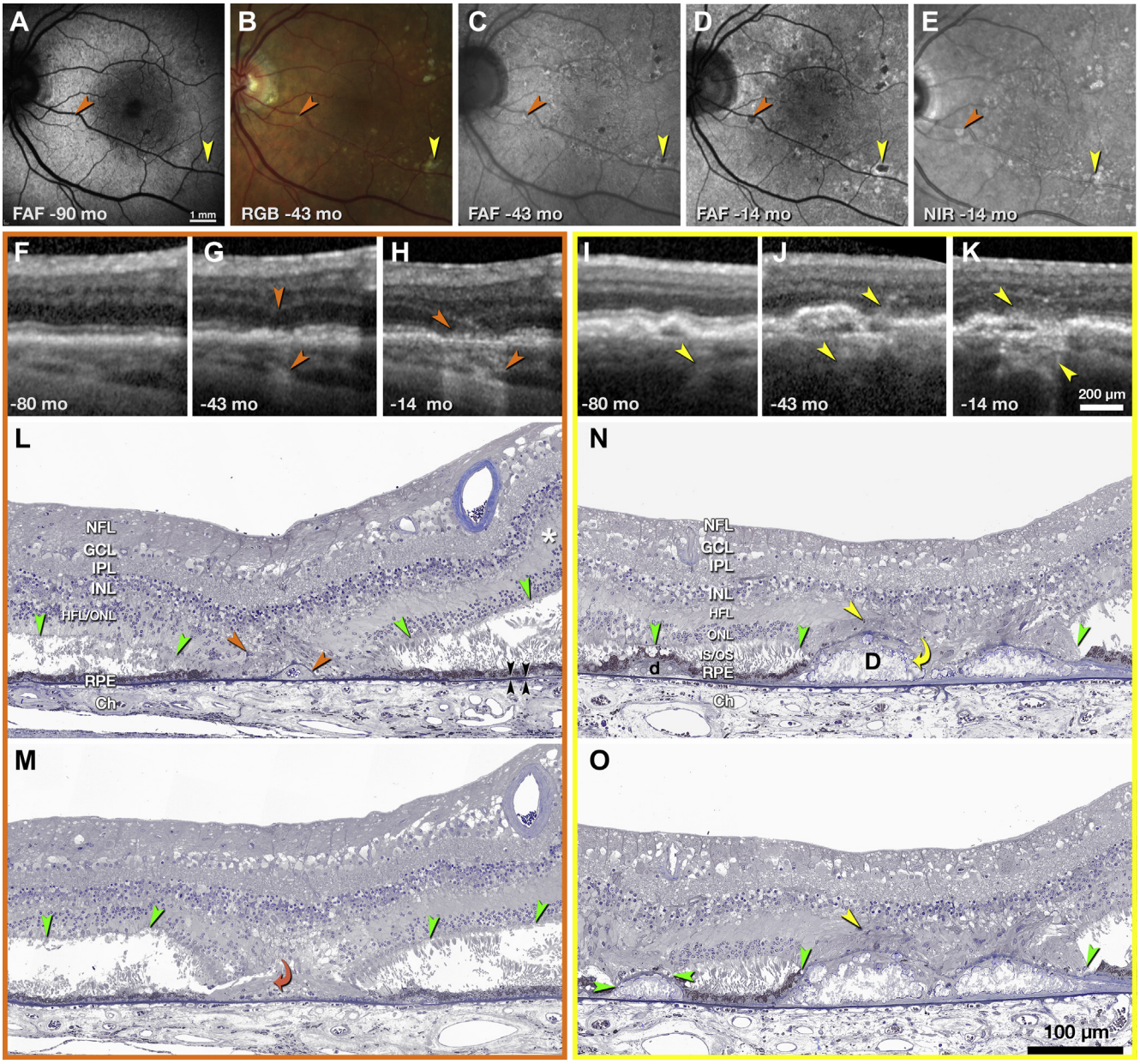

Figure 5. Images showing the evolution and clinicopathologic correlation of druse-associated atrophy. Time points of clinical images are shown as months before the death of this 90-year-old white woman. **A**–**E**, En face imaging showing developing atrophic spots (orange and yellow arrowheads). **F**–**K**, OCT B-scans through the orange (**F**–**H**) and yellow (**I**–**K**) atrophic spots, respectively. Upper and lower arrowheads in (**G**) and (**H**) and in (**I**) and (**J**) indicate hyperreflectivity corresponding to gliosis and hypertransmission into the choroid, respectively. **L**–**N**, Histologic sections through yellow and orange atrophic spots. In atrophic areas, retina is attached to posterior tissues. Outside atrophic areas, artifactual bacillary layer detachment is present. The HFL, in areas of minimal photoreceptor degeneration (asterisk in L), is pale-stained and ordered. In areas of photoreceptor loss, the Henle fiber layer (HFL) is stained medium gray, with disordered fibers and evidence of Müller cell bodies (orange and yellow arrowheads) signifying gliosis. Green arrowheads indicate external limiting membrane (ELM). Black arrowheads indicate Bruch's membrane. **L**, **M**, Histologic sections 60 µm apart through the orange atrophic spot. In (**L**) is a base-down triangle of gliosis (upper arrowhead) and an area of absent outer nuclear layer (ONL) bounded by 2 ELM descents. The prior presence of a druse is indicated by calcific nodules under a blue-stained line of persistent basal laminar deposit (BlamD; **L** lower arrowhead). **M**, The curved arrowhead indicates where processes from the HFL enter under the BLamD. **N**, **O**, Two histologic sections 30 µm apart through the yellow atrophic spot. In the center are 2 drusen (D) with absent retinal pigment epithelium (RPE) and containing large calcific nodules. Through an interruption in the BLamD, gliotic processes enter from the HFL (**N**, yellow curved arrow). In the HFL are presumed Müller cell bodies (**N** and **O**, yellow arrowheads). **N,** There is a small druse (d) on the left side with continuous RPE and ELM. **O**, The ELM has descended onto the druse apex, which is covered with persistent BLamD. The RPE is absent. Ch = choroid; FAF = fundus autofluorescence (excitation wavelengths, 488, 535–585, and 532 nm in (**A**), (**C**), and (**D**), respectively); GCL = ganglion cell layer; INL = inner nuclear layer; IPL = inner plexiform layer; IS/OS = inner and outer segments; NFL = nerve fiber layer; NIR = near-infrared reflectance; OPL = outer plexiform layer; RGB = color photograph. Prepared by J. D. Messinger, DC, and L. Chen, MD, PhD.

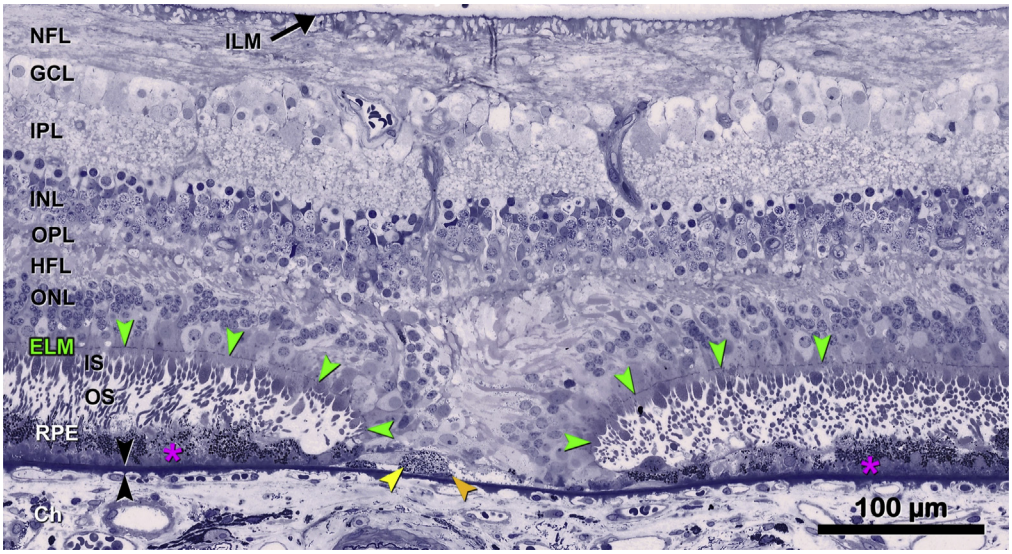

Figure 6. Photomicrograph showing the descent of the external limiting membrane (ELM; green arrowheads) toward Bruch's membrane in an 87-year-old white male donor. The histologic results support the clinical imaging in Figures 2 and 3, bottom row. The ELM descends in 2 curved lines on either side of a narrow isthmus of atrophy typically seen in incomplete retinal pigment epithelium and outer retinal atrophy. The outer nuclear layer (ONL), Henle fiber layer (HFL), outer plexiform layer (OPL), and inner nuclear layer (INL) subside in parallel to the ELM, creating a funnel. The ONL is discontinuous, and the HFL is disordered. Where these ELM descents curve, surviving cone photoreceptors lack outer segments and have short inner segments. Black arrowheads indicate Bruch's membrane (**pink asterisks**, basal laminar **deposit**). ChC = choriocapillaris; GCL = ganglion cell layer; ILM = inner limiting membrane; IPL = inner plexiform layer; NFL = nerve fiber layer. Prepared by M. Li, MD, PhD, and J. D. Messinger, DC, from the Project MACULA age-related macular degeneration histopathology resource (http://projectmacula.cis.uab.edu/).

druse in Figure 2 is associated with hyperreflective foci at its apex, with increasing hypertransmission before the development of iRORA at 6 and 12 months, with subsequent progression to cRORA at 18 months. In Figure 3, the druse at baseline already is associated with hypertransmission of the signal into the choroid and progresses to iRORA at 6 months, with an obvious hyporeflective wedge within the HFL. At 30 months of follow-up, cRORA is established.

Histologic Correlate of Incomplete Retinal Pigment Epithelium and Outer Retinal Atrophy

Figures 4, 5, and 6 present histologic results that support the clinical imaging in Figures 1, 2, and 3. Figure 4 illustrates a large druse in a donor eye with GA where photoreceptor outer segments are absent and inner segments are markedly shortened, and thus, the ELM approaches the druse apex. At the druse apex, RPE is dysmorphic or absent. These histologic findings correlate with the clinical appearance of photoreceptor loss, seen as degradation and thinning of photoreceptor-attributable bands (HFL−ONL, ELM, EZ, and IZ) in Figures 1, 2, and 3. Figure 5 shows histologic results of drusen-associated atrophy (Fig 5L−O) and clinical imaging documenting the development of atrophy over almost 7 years (Fig 5F−K). The appearance of hypertransmission on OCT preceded (Fig 5G) or accompanied (Fig 5J) atrophy on FAF imaging (Fig 5A,C,D). By histologic analysis (Fig 5L,M), the ONL and RPE are absent in an area that is delimited on both sides by 2 ELM descents. Within the area of atrophy, tombstone markers of a prior druse are persistent basal laminar deposits overlying calcific nodules. In Figure 5N,O, an atrophic spot on each druse apex includes photoreceptor degeneration (i.e., absent inner and outer segments). A profound finding on histologic analysis is significant gliosis associated with each atrophic area (Fig 5M−O). This may be recognizable on OCT by increased reflectivity of the normally hyporeflective HFL. Figure 6 provides a high-magnification view of the ELM descending toward Bruch's membrane in 2 curved lines bounding a narrow isthmus of atrophy. The HFL, OPL, and INL subside between the 2 ELM descents, creating a funnel. Hyporeflective wedges in the HFL have been correlated histologically to parallel Henle fibers without cellular infiltration that are permissive to transmitted light on the same axis.[32] The ONL descends in parallel with the ELM and is absent in the atrophic area. Along the ELM descents, the remaining cone photoreceptors are oriented horizontally, lack outer segments, and have short inner segments.

Variability in the Sequence of Anatomic Changes Seen in Early Atrophy

With OCT imaging, cases of early atrophy may be identified where some iRORA signs are absent and cases in which the near-infrared reflectance, FAF, and CFP images do not always corroborate these signs of atrophy. This variability may be important in representing different phenotypes with different natural histories and disease severity (Figs 7−9). In Figure 7, OCT imaging illustrates loss of the outer retina and increasing disruption of the RPE layer, followed by loss of the RPE layer and increasing hypoautofluorescence on FAF imaging. However, the extent of

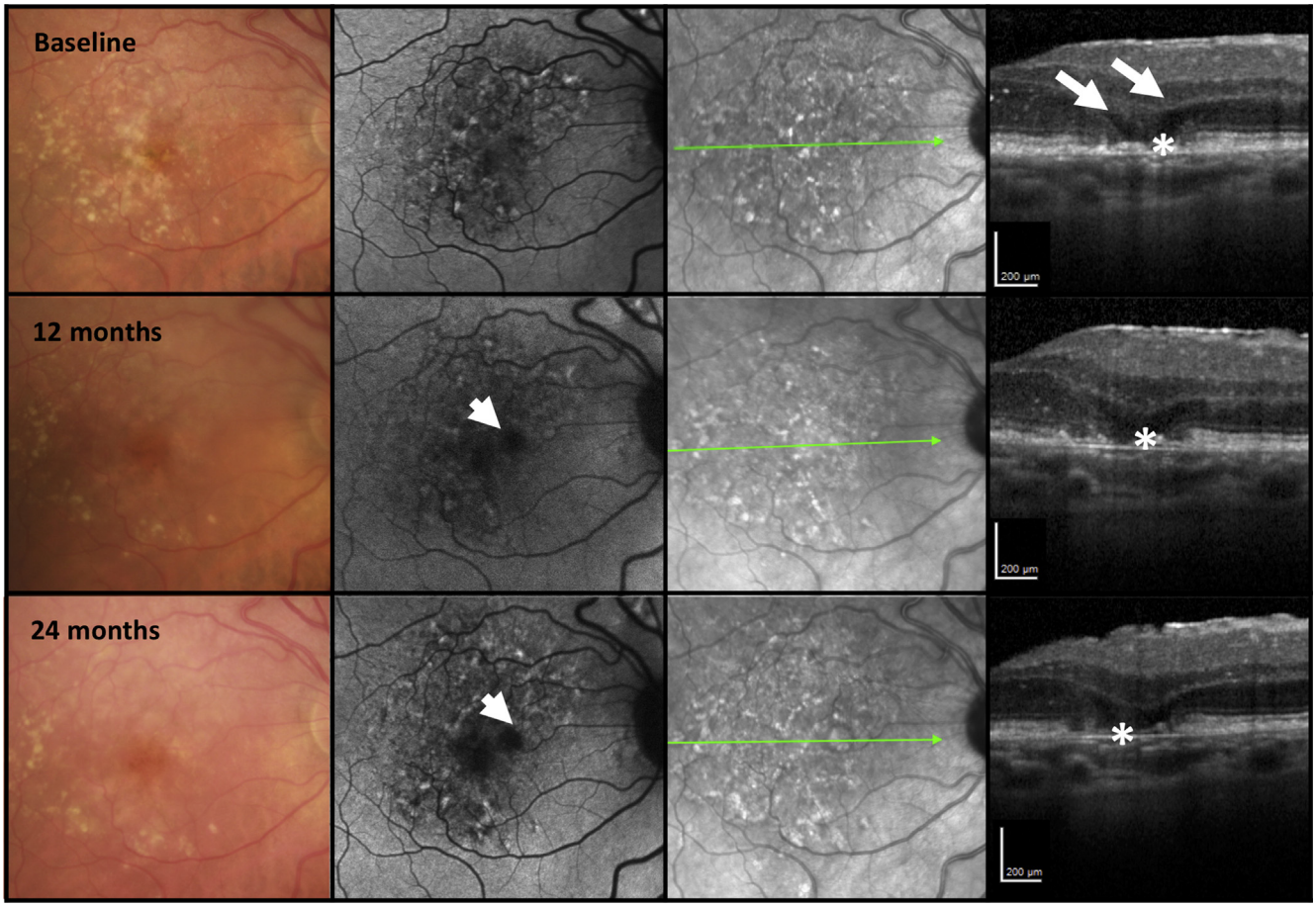

Figure 7. Multimodal imaging of an age-related macular degeneration case illustrating retinal pigment epithelium loss without choroidal hypertransmission over 24 months: color fundus photography (CFP; first column), fundus autofluorescence (FAF; second column), near-infrared reflectance (NIR; third column), and OCT B-scan (fourth column). The right macula of a case demonstrating large drusen and pigmentary abnormalities is shown on CFP. At baseline, the FAF demonstrates a mottled hypoautofluorescent and hyperautofluorescent signal. The NIR also presents a mottled reflectance. The OCT demonstrates minimal subsidence of the inner nuclear layer and outer plexiform layer but obvious hyporeflective wedges in the Henle fiber layer (large arrows). Retinal pigment epithelium (RPE) attenuation (asterisk) without obvious hypertransmission into the choroid is evident. At 12 and 24 months, although increasing hypoautofluorescence is present on FAF imaging and progressive loss of the RPE (asterisk) and a bare Bruch's membrane, minimal hypertransmission into the choroid is evident on the OCT, where greater hypertransmission would be expected to accompany the RPE loss. At no point in this illustration were all the criteria met for incomplete RPE and outer retinal atrophy.

hypertransmission into the choroid, which should depend on the disruption of the RPE layer, does not appear commensurate with the baring of Bruch's membrane. As such, at no time in this example would the definition of iRORA be met. Figure 8 at baseline demonstrates a collapsing druse with outer retinal loss, attenuation of the RPE, and hypertransmission, and therefore meets the definition of iRORA. However, at 6 months, the RPE appears intact in the same area as the collapsed druse, appearing similar to adjacent RPE. Significant hypertransmission into the choroid can be appreciated, despite the apparent relatively intact RPE layer. Given the intact RPE, at this later time point, iRORA criteria are not met.

In Figure 9, a case of AMD is presented with a druse displaying hypertransmission at baseline. Loss of some outer retinal layers is apparent, but the RPE is preserved, thus not fulfilling all criteria for iRORA. At 6 months, the druse appears nonreflective, but the overlying RPE remains intact (with basal laminar deposits), yet there is hypertransmission of the signal into the choroid. All criteria for iRORA are still not met. Over time, the druse contour persists, and there is internal reflectivity within the druse, with persistent and striking hypertransmission (24 months). At 24 months, the RPE is attenuated, and as such, iRORA now is present. Despite the hypertransmission, there is no obvious hypofluorescence on the FAF image (second column), although the luteal pigment could hinder recognition of this change. Color fundus photography-defined GA also is not identified.

Incomplete Retinal Pigment Epithelium and Outer Retinal Atrophy Screening

Although the CAM group focused primarily on the analysis of single individual OCT B-scans to define characteristic features of iRORA, en face sub-RPE OCT slabs may be used as a screening tool to detect choroidal hypertransmission

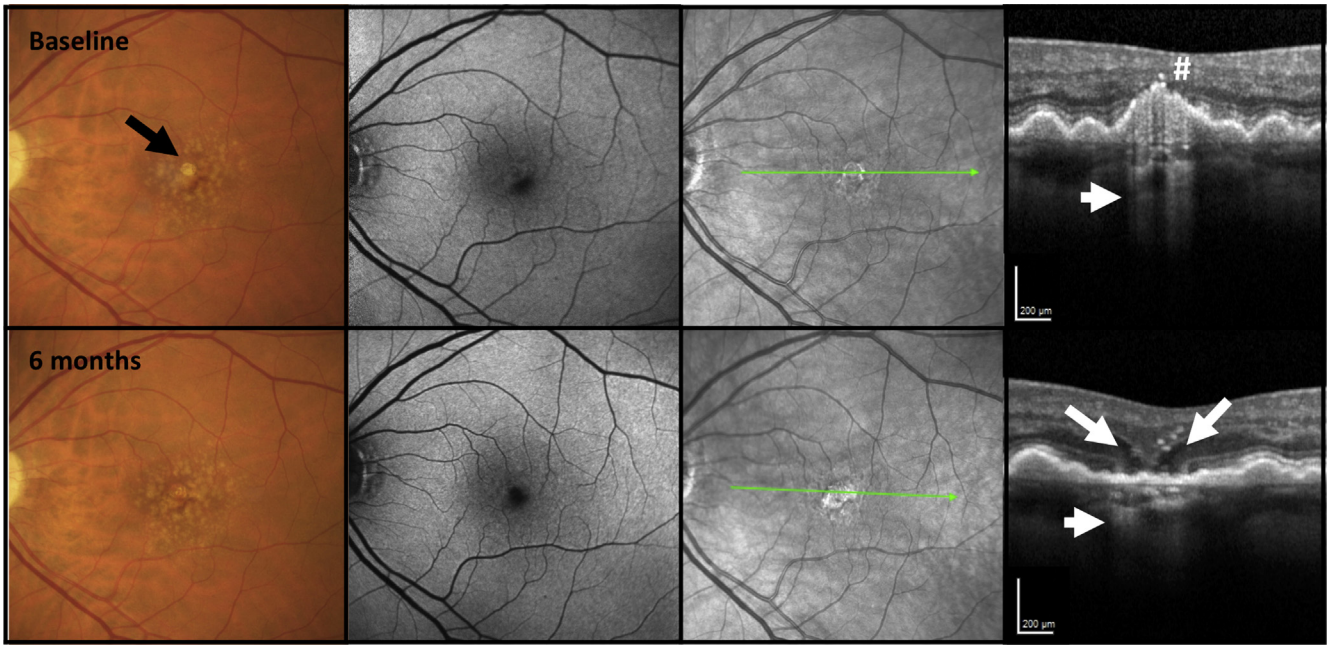

Figure 8. Multimodal imaging of an age-related macular degeneration (AMD) case illustrating choroidal hypertransmission despite apparent presence of the retinal pigment epithelium (RPE): color fundus photography (CFP; first column), fundus autofluorescence (FAF; second column), near-infrared reflectance (NIR; third column), and OCT B-scan (fourth column). The left macula of a case of intermediate AMD illustrating large drusen and pigment disturbance, including one area of hypopigmentation (black arrow) not obvious on FAF but seen as a circumscribed area on NIR. At baseline, the OCT demonstrates a large druse with hyperreflective foci (number sign) at the druse apex and hypertransmission into the choroid (small arrow) in a so-called bar code appearance. The RPE is attenuated. There is no subsidence of the inner nuclear layer and outer plexiform layer (OPL), although the outer nuclear layer (ONL) is thinned and the external limiting membrane (ELM) and ellipsoid zone are discontinuous. At baseline, all criteria for incomplete RPE and outer retinal atrophy (iRORA) have been met. At 6 months, the druse has regressed, and 2 hyporeflective wedges in the Henle fiber layer, subsidence of the OPL and ONL, and a descent of the ELM bounding both sides of the atrophy (large arrows) are present. However, the RPE now appears to remain intact, although hypertransmission clearly is present (small arrow). As such, at this time point, all the criteria for iRORA are not met. Because the CFP image has a corresponding area of hypopigmentation, one explanation for this RPE appearance is preferential loss of melanosomes from the RPE that reduces (but does not eliminate) backscatter.

associated with iRORA, which then could be confirmed with the corresponding B-scans. The specificity and sensitivity of en face imaging as a screening tool remains to be determined (Figs 10 and 11).[26,33] In Figure 10, a case with large drusen is shown in Figure 10A, B, in which a custom slab en face structural swept-source OCT image illustrates bright areas corresponding to the hypertransmission signal. These areas are associated with loss of photoreceptor attributable bands (although difficult to appreciate directly beneath the fovea). Because no clear RPE attenuation or disruption is visible, the criteria for iRORA have not been meet. Six months later, in Figure 10D, a small disruption in the RPE is seen, and iRORA criteria are meet. In Figure 11, the case illustrates drusen with baseline en face structural images that initially display a dark area that corresponds to anterior pigment migration over a druse (Fig 11D). With time, the follow-up en face structural image shows a bright area (Fig 11B) that corresponds to the druse associated with a subtle hypertransmission signal into the choroid, subsidence of the INL and OPL, and attenuation of the RPE, fulfilling all the criteria for iRORA in Figure 11 E, F.

Discussion

A consensus nomenclature and definition for atrophy based on OCT imaging was proposed by the CAM Group. The terms *iRORA* and *cRORA* are defined, both in this and our prior report,[31] to describe the evolution of atrophy in AMD. For iRORA to be present, 3 OCT features are required to be present and vertically aligned: signs of photoreceptor degeneration, RPE attenuation or disruption, and increased signal transmission into the choroid. If the areas of RPE change and hypertransmission each have a diameter of at least 250 µm on the OCT B-scan, in addition to evidence of photoreceptor loss, then they qualify as cRORA. A minimum size limit for iRORA was not proposed, and the ability of reading centers to identify the constellation of iRORA signs reproducibly is not yet known. The aim of this article is to provide criteria and nomenclature for cell loss as seen on OCT. As discussed next, it is now imperative to determine how reliably specific features of iRORA can be graded and their usefulness in predicting progression.

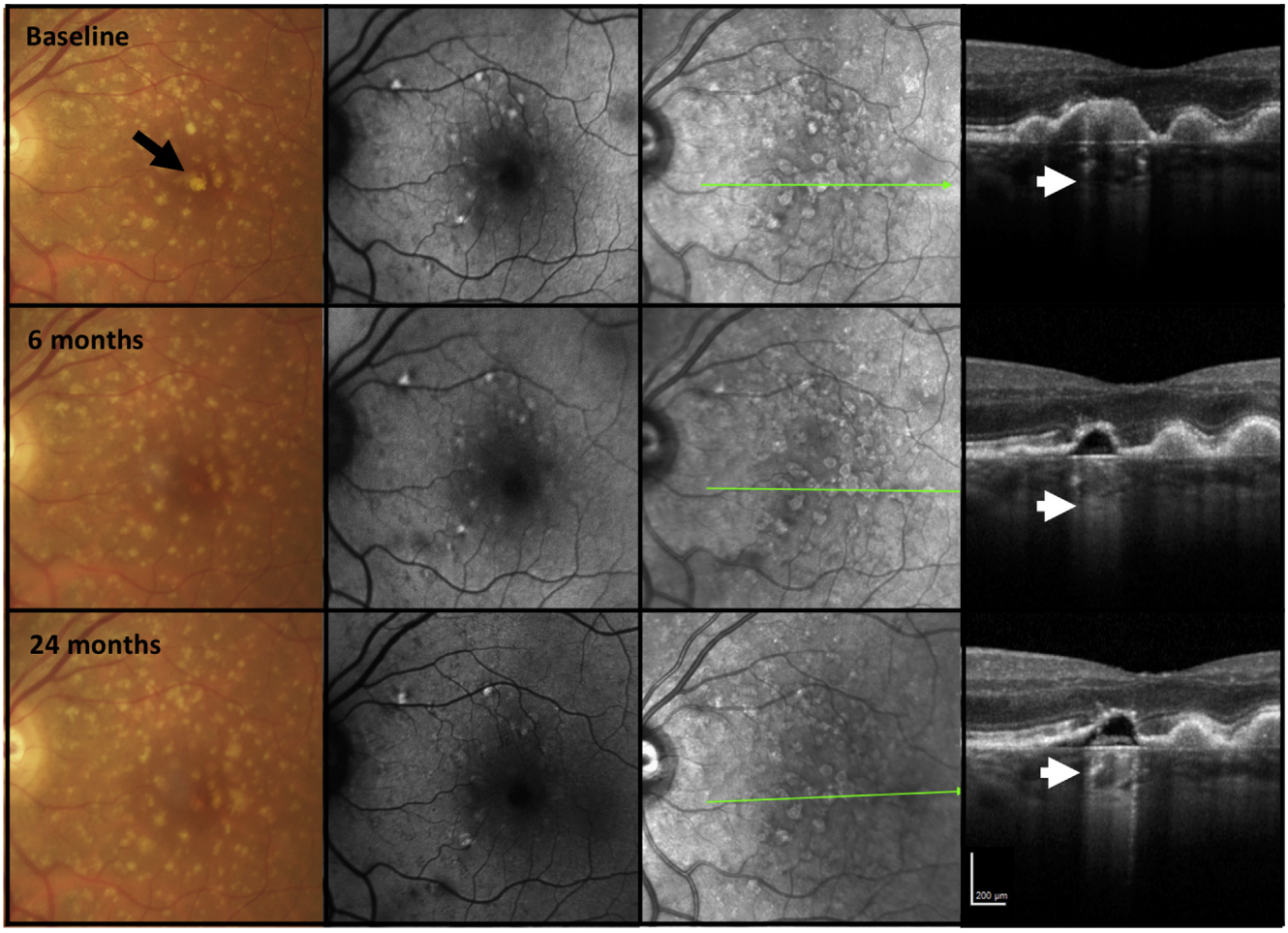

Figure 9. Multimodal imaging of an age-related macular degeneration case illustrating marked choroidal hypertransmission despite relatively intact retinal pigment epithelium (RPE) and persistence of the druse contour: color fundus photography (CFP; first column), fundus autofluorescence (FAF; second column), near-infrared reflectance (NIR; third column), and OCT B-scan (fourth column). The left macula of a case illustrating large drusen on CFP with some hypopigmentation at baseline (black arrow). Fundus autofluorescence and NIR do not demonstrate areas of hypoautofluorescence on FAF or reduced NIR, respectively. On OCT at baseline, a druse displays hypertransmission into the choroid (bar code appearance, white arrow). There is no subsidence of the the inner nuclear layer or outer plexiform layer, and the RPE is preserved, thus not fulfilling all criteria for iRORA. At 6 months, the druse has reduced in size and appears hyporeflective, but the overlying RPE remains intact above it, yet there is hypertransmission of the signal into the choroid (small arrow). All the criteria for incomplete RPE and outer retinal atrophy (iRORA) are still not met. Over time, the druse contour and marked hypertransmission persist (small arrow), and internal reflectivity partially fills the druse. The RPE is now becoming attenuated, although still with potentially residual basal laminar deposit. At 24 months, all the criteria for iRORA have been met. Despite the hypertransmission, no obvious hypoautofluorescence is present on FAF, although this area is masked by luteal pigment. No hyporeflective areas are seen on NIR, nor is there any corresponding geographic atrophy on CFP.

Using case examples with longitudinal follow-up in eyes with drusen (Figs 2 and 3), we provide evidence that the features of iRORA predict development of cRORA. These case studies demonstrate the spectrum of OCT signs that indicate photoreceptor degeneration, RPE disruption or attenuation, and hypertransmission of the signal into the choroid. Reproducibility for identifying iRORA is crucial and undoubtedly will improve as clinicians and reading centers become more familiar with the OCT findings as well as with advances in OCT technology and adoption of artificial intelligence algorithms as they become available.

The CAM group believed that the term *GA*, well entrenched in the AMD nomenclature, but with several current CFP definitions, should remain and continue to be used as a term applied to the subset of cRORA occurring in the absence of current or past macular neovascularization. Similarly, the term *nGA* should be used more broadly when iRORA is present in the absence of current or prior macular neovascularization, signifying that progression toward GA has begun.[23,24] This is a slight modification from its original OCT description, which required subsidence of the INL and OPL or a hyporeflective wedge-shaped band within the HFL as evidence of photoreceptor loss, and although usual to see RPE change and hypertransmission, they were not mandatory.[23,24]

It is recognized that even before all 3 criteria of iRORA are present (photoreceptor and RPE degradation with hypertransmission), there will be OCT scans in which some, but not all, signs are present. These eyes should be considered as having risk factors for the progression to

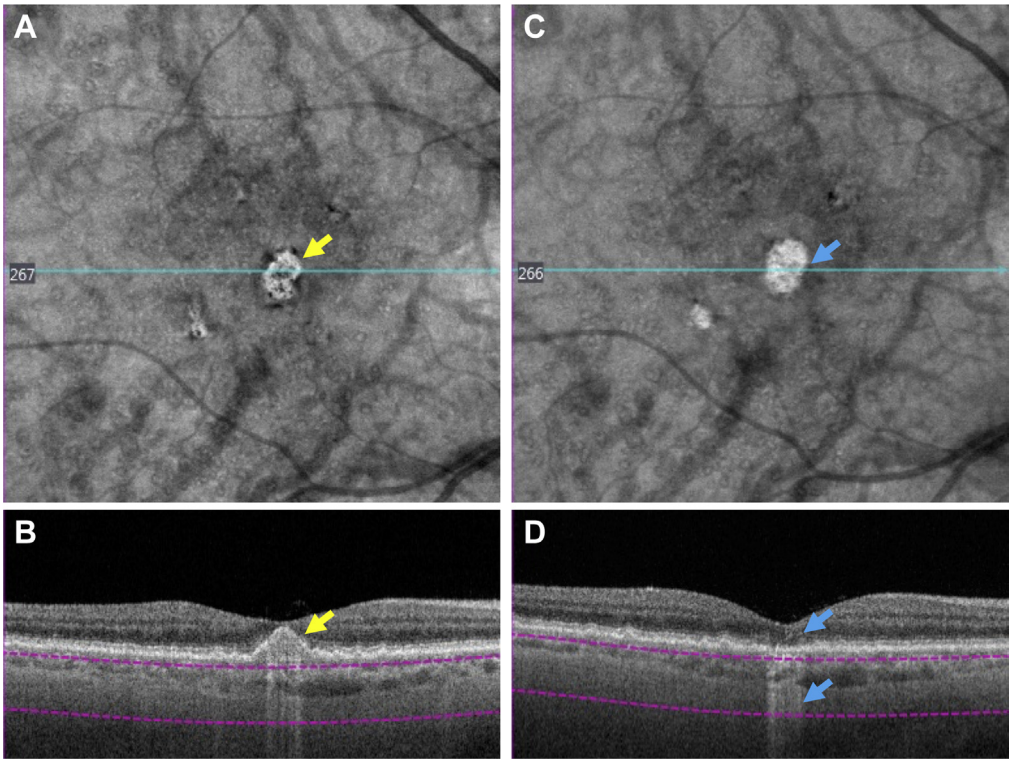

Figure 10. Screening for incomplete retinal pigment epithelium (RPE) and outer retinal atrophy (iRORA) using an en face slab with boundaries beneath the RPE to detect hypertransmission into the choroid using swept-source (SS) OCT imaging: 6×6-mm SS OCT angiography images of a right eye with large drusen, with (**A**) and (**B**) depicting the eye at baseline and (**C**) and (**D**) showing progression after 6 months. **A**, En face structure image using custom sub-RPE slab depicted by the purple boundary lines in (**B**), and the bright area (yellow arrow) corresponds to the area of hypertransmission shown in (**B**). **B**, Swept-source OCT B-scan showing a large druse with hypertransmission (yellow arrow). The boundary lines for the sub-RPE slab are shown beneath the RPE. Loss of the photoreceptor-attributable bands is evident, but the RPE remains intact, and as such, criteria for iRORA have not been met. **C**, Six months later, an en face structure image using the same custom sub-RPE slab depicted in panel (**A**) but with a brighter area (blue arrow) corresponding to the area of hypertransmission shown in (**D**). **D**, Swept-source OCT B-scan showing the collapse of the large druse with hypertransmission (lower blue arrow), disruption of the outer retinal layers (upper blue arrow), and a small disruption in the RPE can be seen. All criteria for iRORA have been reached.

iRORA but have not yet reached iRORA. They are added to a constellation of other OCT signs, such as intraretinal hyperreflective foci, heterogeneous internal reflectivity of drusen, and subretinal drusenoid deposits, that may be considered as high-risk OCT biomarkers for progression.[12–22] These risk factors for progression to iRORA will be explored in planned future publications by the CAM Group. The importance attributed to the degradation of each layer or band will become more evident as longitudinal studies accrue detailed grading on each of these changes. As such, the relative weight placed on each individual layer or zone's degradation as a predictor of progression to vision loss will become more apparent. Currently, detection of these signs involves the inspection of single OCT B-scans but can be facilitated by screening with en face OCT imaging to detect the choroidal hypertransmission signal (Figs 10 and 11).[26,33] It is the hope of the CAM Group that researchers will apply these definitions and determine the progression rates from iRORA to cRORA and the robustness of en face screening and assess the relative contribution of iRORA components as predictive biomarkers of progression.

With greater knowledge of individual signs and their association with disease progression, it will be possible to inform artificial intelligence algorithms to develop robust models to predict progression. Determining the rate of progression from iRORA to cRORA will be important information when considering the design of new interventional studies to prevent the development of atrophy. Thereafter, a possible way to show efficacy of a therapeutic intervention to slow or halt progression from iRORA to cRORA in clinical trials is to demonstrate alteration of this progression trajectory. The Food and Drug Administration has suggested that the onset of atrophy, if able to be measured precisely and reproducibility, could be acceptable as a trial end point.[4] In a recent intervention trial of subthreshold laser in participants with bilateral large drusen, progression to nGA was used as an outcome measure, providing initial support for nGA as a surrogate end point for GA.[34]

Photoreceptor cells contribute to multiple bands of alternating reflectivity in OCT images: OPL (synaptic terminals), HFL (axonal fibers), ONL (cell bodies), ELM (junctions with Müller glia), EZ (outer part of photoreceptor

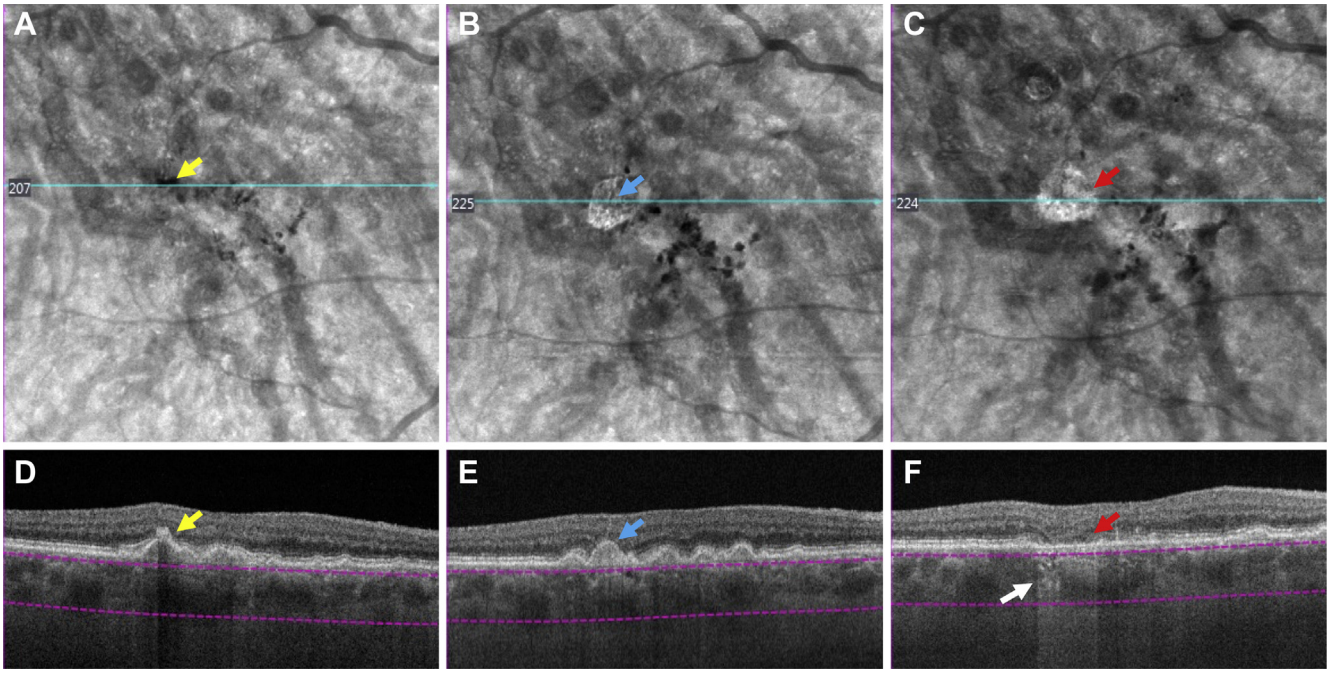

Figure 11. Screening for incomplete retinal pigment epithelium (RPE) and outer retinal atrophy (iRORA) using an en face slab with boundaries beneath the RPE to detect both hypotransmission and hypertransmission into the choroid using swept-source (SS) OCT imaging: 6×6-mm SS OCT angiography images in an eye with large drusen, with (**A**) and (**D**) representing the baseline visit, (**B**) and (**E**) represent the 12-month follow-up visit, and (**C**) and (**F**) representing the 20-month follow-up visit, where iRORA is evident (red arrow). **A**, En face structural image using a custom slab (purple lines) showing a hyporeflective area (yellow arrow) corresponding to pigment migration (hyperreflective foci) over the druse in (**D,** yellow arrow). **B**–**F**, En face structure images using a custom slab showing a hyperreflective area (**B,** blue arrow and **C,** red arrow), which respectively corresponds to drusen (**E,** blue arrow) with hypertransmission (**F,** white arrow), subsidence of the inner nuclear layer (INL) and outer plexiform layer (OPL), and a faint wedge-shaped band in the Henle fiber layer (red arrow). In (**E**), subtle hypertransmission into the choroid, subsidence of the INL and OPL, and attenuation of the RPE are present, fulfilling all the criteria for iRORA, and again in (**F**), iRORA is present, and the druse has regressed completely.

inner segments), outer segments, and IZ (interface of outer segments with RPE apical processes). Müller glia also participate in the first 4 of these bands. Clinically, we infer photoreceptor health based on the integrity of these bands. An important question is whether changes or disruption in any of these bands indicate an irreversible commitment to photoreceptor cell degeneration or whether therapies still can rescue them. In surgically repaired macular holes, it is possible to see reversal of some preoperative interruption in the ELM and EZ. The re-establishment of a continuous EZ and ELM band in the postoperative phase correlates with visual acuity improvement,[35,36] in which the extent of preoperative EZ and ELM interruption may be a determining factor in the gain of visual acuity.[37] Whether this amelioration in the morphologic changes in the ELM and EZ anatomic features could occur in the context of evolving atrophic AMD is not known.

Another important consideration in the study of atrophy is the intense gliosis of Müller cells that accompanies photoreceptor degeneration and loss. Recent histologic studies of GA have highlighted the role of Müller cells in dyslamination of the combined HFL and ONL (i.e., loss of clear laminar boundaries), formation of the ELM descent and glial scars, and Müller cell persistence after photoreceptor depletion, all of which complicate the task of quantifying photoreceptor abundance and health.[38–40] The ELM descent occurs in advance of degeneration in the RPE–Bruch's membrane complex, a process that is hypothesized as Müller cells barricading the surviving photoreceptors from factors present in the damaged atrophic zone.[41] Herein, we show that the ELM descends on top of individual druse along with RPE loss (Fig 5). Because of the precise arrangement of cells that comprise the normally hyporeflective HFL and ONL, it may be possible to recognize reflectivity changes accompanying gliosis in this layer on OCT (Fig 5). Exploring HFL and ONL intensity as a predictor of atrophy expansion thus may have merit.[42]

Limitations of our study include the case-based nature of our analysis that may have biased our conclusions. The overall rate of transition from iRORA to cRORA and the proportion of eyes in which this transition occurs is not yet known and requires large prospective studies. However, the purpose of this report, which builds on the CAM 3 report,[31] is to establish a framework around which researchers can move forward to fill in these critical knowledge gaps. We also recognize that the constellation of anatomic signs that we describe are not an absolute, all-or-none phenomena; cases of atrophy can occur through other pathways.[43] In many cases of drusen-associated atrophy, we believe the anatomic changes follow the described pathway. Our strength is that a group of experts came to a consensus for signs that we hypothesize indicate that the path to atrophy has begun, with an increased risk of vision loss resulting

from late AMD. The Food and Drug Administration has indicated that it looks to the scientific community for consensus as to when a significant biomarker of disease progression has been reached.[4] Creating a path forward to allow further definition of this risk through well-designed clinical studies is essential to satisfy the regulatory authorities and to keep industry collaborators engaged in AMD research, ultimately leading to the development of new AMD therapeutics.

In conclusion, an international consensus classification system and criteria for OCT-defined anatomic changes that occur before GA has been advanced, with iRORA described both clinically and pathologically and case examples of longitudinal progression to cRORA provided. Future studies are needed to determine our ability to identify these signs reproducibly and to provide the progression rates from iRORA to cRORA, facilitating their use as robust outcome measures applicable in the design of clinical trials. Although there is still much to learn about the longitudinal history of AMD based on natural history studies and histopathologic features, the proposed consensus nomenclature will find application in studies such as the large European MACUSTAR program.[44] Consideration of these features will be essential for designing interventional trials for treatments that aim to slow progression, because they are potential confounders.

References

1. Bird AC, Bressler NM, Bressler SB, et al. An international classification and grading system for age-related maculopathy and age-related macular degeneration. The International ARM Epidemiological Study Group. *Surv Ophthalmol*. 1995;39:367−374.
2. Schmitz-Valckenberg S. The journey of "geographic atrophy" through past, present, and future. *Ophthalmologica*. 2017;237:11−20.
3. Ferris 3rd FL, Wilkinson CP, Bird A, et al. Clinical classification of age-related macular degeneration. *Ophthalmology*. 2013;120:844−851.
4. Csaky K, Ferris III F, Chew EY, et al. Report from the NEI/FDA Endpoints Workshop on age-related macular degeneration and inherited retinal diseases. *Invest Ophthalmol Vis Sci*. 2017;58:3456−3463.
5. Holz FG, Strauss EC, Schmitz-Valckenberg S, et al. Geographic atrophy: clinical features and potential therapeutic approaches. *Ophthalmology*. 2014;121:1079−1091.
6. Schmitz-Valckenberg S, Sahel JA, Danis R, et al. Natural history of geographic atrophy progression secondary to age-related macular degeneration (Geographic Atrophy Progression Study). *Ophthalmology*. 2016;123:361−368.
7. Cheng QE, Gao J, Kim BJ, Gui-shuang Ying G. Design characteristics of geographic atrophy treatment trials: systematic review of registered trials in ClinicalTrials.gov. *Ophthalmol Retina*. 2018;2:518−525.
8. Holz FG, Sadda SR, Busbee B, et al. Efficacy and safety of lampalizumab for geographic atrophy due to age-related macular degeneration Chroma and Spectri phase 3 randomized clinical trials. *JAMA Ophthalmol*. 2018;136(6):666−677.
9. Rosenfeld PJ, Dugel PU, Holz FG. Emixustat hydrochloride for geographic atrophy secondary to age-related macular degeneration: a randomized clinical trial. *Ophthalmology*. 2018;125:1556−1567.
10. Guymer RH. Geographic atrophy trials: turning the ship around may not be that easy. *Ophthalmology*. 2018;2:515−517.
11. Age-Related Eye Disease Study Group. The Age-Related Eye Disease Study system for classifying age-related macular degeneration from stereoscopic color fundus photographs: the Age-Related Eye Disease Study report number 6. *Am J Ophthalmol*. 2001;132:668−681.
12. Abdelfattah NS, Zhang H, Boyer DS, et al. Drusen volume as a predictor of disease progression in patients with late age-related macular degeneration in the fellow eye. *Invest Ophthalmol Vis Sci*. 2016;57:1839−1846.
13. Veerappan M, El-Hage-Sleiman AM, Tai V, et al. Optical coherence tomography reflective drusen substructures predict progression to geographic atrophy in age-related macular degeneration. *Ophthalmology*. 2016;123:2554−2570.
14. Tan AC, Pilgrim M, Fearn S, et al. Calcified nodules in retinal drusen are associated with disease progression with age-related macular degeneration. *Sci Transl Med*. 2018;10(466). pii: eaat4544 https://doi: 10.1126/scitranslmed.aat4544.
15. Christenbury JG, Folgar FA, O'Connell RV, et al. Progression of intermediate age-related macular degeneration with proliferation and inner retinal migration of hyperreflective foci. *Ophthalmology*. 2013;120:1038−1045.
16. Ouyang Y, Heussen FM, Hariri AH, et al. Optical coherence tomography−based observation of the natural history of drusenoid lesion in eyes with dry age-related macular degeneration. *Ophthalmology*. 2013;120:2656−2665.
17. Ferrara D, Silver RE, Louzada RN, et al. Optical coherence tomography features preceding the onset of advanced age related macular degeneration. *Invest Ophthalmol Vis Sci*. 2017;58:3519−3529.
18. Curcio CA, Zanzottera EC, Ach T, et al. Activated retinal pigment epithelium, an optical coherence tomography biomarker for progression in age-related macular degeneration. *Invest Ophthalmol Vis Sci*. 2017;58:BI0211−BI0226.
19. Zweifel SA, Spaide RF, Curcio CA, et al. Reticular pseudodrusen are subretinal drusenoid deposits. *Ophthalmology*. 2010;117:303−312.
20. Finger RP, Wu Z, Luu CD, et al. Reticular pseudodrusen. A risk factor for geographic atrophy in fellow eyes of individuals with unilateral choroidal neovascularization. *Ophthalmology*. 2014;121:1252−1256.
21. Zweifel SA, Imamura Y, Spaide TC, et al. Prevalence and significance of subretinal drusenoid deposits (reticular pseudodrusen) in age-related macular degeneration. *Ophthalmology*. 2010;117:1775−1781.
22. Schmitz-Valckenberg S, Alten F, Steinberg JS, et al. Reticular drusen associated with geographic atrophy in age-related macular degeneration. *Invest Ophthalmol Vis Sci*. 2011;52:5009−5015.
23. Wu Z, Luu CD, Ayton LN, et al. Optical coherence tomography-defined changes preceding the development of drusen-associated atrophy in age-related macular degeneration. *Ophthalmology*. 2014;121:2415−2422.
24. Wu Z, Luu CD, Ayton LN, et al. Fundus autofluorescence characteristics of nascent geographic atrophy in age-related macular degeneration. *Invest Ophthalmol Vis Sci*. 2015;56:1546−1552.
25. Monés J, Biarnés M, Trindade F. Hyporeflective wedgeshaped band in geographic atrophy secondary to age-related macular degeneration: an underreported finding. *Ophthalmology*. 2012;119:1412−1419.
26. Schaal KB, Gregori G, Rosenfeld PJ. En face optical coherence tomography imaging for the detection of

nascent geographic atrophy. *Am J Ophthalmol*. 2017;174:145–154.
27. Choi W, Moult EM, Waheed NK, et al. Ultrahigh-speed, swept-source optical coherence tomography angiography in nonexudative age-related macular degeneration with geographic atrophy. *Ophthalmology*. 2015;122(12):2532–2544.
28. Nassisi M, Shi Y, Fan W, et al. Choriocapillaris impairment around the atrophic lesions in patients with geographic atrophy: a swept-source optical coherence tomography angiography study. *Br J Ophthalmol*. 2019;103(7):911–917.
29. Schmitz-Valckenberg S, Sadda S, Staurenghi G, et al. Semantic considerations and literature review. *Retina*. 2016;36(12):2250–2264.
30. Holz FG, Sadda SR, Staurenghi G, et al. Imaging protocols in clinical studies in advanced age-related macular degeneration: recommendations from Classification of Atrophy Consensus Meetings. *Ophthalmology*. 2017;124:464–478.
31. Sadda SR, Guymer R, Holz FG, et al. Consensus definition for atrophy associated with age-related macular degeneration on OCT: Classification of Atrophy report 3. *Ophthalmology*. 2017;125(4):537–548.
32. Li M, Dolz-Marco R, Huisingh C, et al. Clinicopathologic correlation of geographic atrophy secondary to age-related macular degeneration. *Retina*. 2019;39(4):802–816.
33. Nunes RP, Gregori G, Yehoshua Z, et al. Predicting the progression of geographic atrophy in AMD with SD-OCT en face imaging of the outer retina. *Ophthalmic Surg Lasers Imaging Retina*. 2013;44:344–359.
34. Guymer RH, Wu Z, Hodgson LAB, et al. Subthreshold nanosecond laser intervention in age-related macular degeneration. The LEAD Randomized Controlled Clinical Trial. *Ophthalmology*. 2019;126(6):829–838.
35. Bottoni F, De Angelis S, Luccarelli S, et al. The dynamic healing process of idiopathic macular holes after surgical repair: a spectral-domain optical coherence tomography study. *Invest Ophthalmol Vis Sci*. 2011;52:4439–4446.
36. Landa G, Gentile RC, Garcia PM, et al. External limiting membrane and visual outcome in macular hole repair: spectral domain OCT analysis. *Eye*. 2012;26:61–69.
37. Guo J, Tang W, Ye X, et al. Predictive multi-imaging biomarkers relevant for visual acuity in idiopathic macular telangiectasis type 1. *BMC Ophthalmol*. 2018;18:69.
38. Dolz-Marco R, Balaratnasingam C, Messinger JD, et al. The border of macular atrophy in age-related macular degeneration: a clinicopathologic correlation. *Am J Ophthalmol*. 2018;193:166–177.
39. Li M, Huisingh C, Messinger JD, et al. Histology of geographic atrophy secondary to age-related macular degeneration: a multilayer approach. *Retina*. 2018;38:1937–1953.
40. Edwards MM, McLeod DS, Bhutto IA, et al. Subretinal glial membranes in eyes with geographic atrophy. *Invest Ophthalmol Vis Sci*. 2017;58:1352–1367.
41. Dolz-Marco R, Litts KM, Tan ACS, et al. The evolution of outer retinal tubulation, a neurodegeneration and gliosis prominent in macular diseases. *Ophthalmology*. 2017;124:1353–1367.
42. Stetson PF, Yehoshua Z, Garcia Filho CA, et al. OCT minimum intensity as a predictor of geographic atrophy enlargement. *Invest Ophthalmol Vis Sci*. 2014;55:792–800.
43. Spaide RF. Outer retinal atrophy after regression of subretinal drusenoid deposits as a newly recognized form of late age-related macular degeneration. *Retina*. 2013;33:1800–1808.
44. Finger RP, Schmitz-Valckenberg S, Schmid M, et al. MACUSTAR: development and clinical validation of functional, structural, and patient-reported endpoints in intermediate age-related macular degeneration. *Ophthalmologica*. 2019;241(2):61–72.

Footnotes and Financial Disclosures

Originally received: March 22, 2019.
Final revision: August 26, 2019.
Accepted: September 24, 2019.
Available online: September 30, 2019. Manuscript no. 2019-634.

[1] Centre for Eye Research Australia, Royal Victorian Eye and Ear Hospital, University of Melbourne, Department of Surgery (Ophthalmology), Melbourne, Australia.

[2] Bascom Palmer Eye Institute, University of Miami Miller School of Medicine, Miami, Florida.

[3] Department of Ophthalmology and Visual Sciences, School of Medicine, University of Alabama at Birmingham, Birmingham, Alabama.

[4] Department of Ophthalmology, University of Bonn, Bonn, Germany.

[5] Eye Clinic, Department of Biomedical and Clinical Sciences "Luigi Sacco," Luigi Sacco Hospital, University of Milan, Milan, Italy.

[6] Vitreous Retina Macula Consultants of New York, New York, New York.

[7] Departments of Ophthalmology and Pathology and Cell Biology, Columbia University Medical Center, New York, New York.

[8] Institute of Ophthalmology, University College London, London, United Kingdom.

[9] Center for Public Health, The Queen's University of Belfast, Belfast, United Kingdom.

[10] Department of Ophthalmology, Duke University, Durham, North Carolina.

[11] Retina Foundation of the Southwest, Dallas, Texas.

[12] Stein Eye Institute, David Geffen School of Medicine, University of California, Los Angeles, Los Angeles, California.

[13] Institut de la Màcula and Barcelona Macula Foundation, Barcelona, Spain.

[14] Department of Ophthalmology, Hôpital Lariboisière, AP-HP, Université Paris 7—Sorbonne, Paris, France.

[15] Department of Ophthalmology, University of Pennsylvania, Philadelphia, Pennsylvania.

[16] Department of Ophthalmology, University of Cologne, Cologne, Germany.

[17] Department of Ophthalmology, St. Franziskus Hospital, Münster, German.

[18] Department of Ophthalmology, University Hospitals Coventry & Warwickshire, Coventry, United Kingdom.

[19] National Eye Institute, National Institutes of Health, Bethesda, Maryland.

[20] Cà Granda Foundation, Ospedale Maggiore Policlinico, University of Milan, Milan, Italy.

[21] Department of Ophthalmology and Visual Sciences, Fundus Photograph Reading Center, University of Wisconsin School of Medicine and Public Health, Madison, Wisconsin.

[22] National Healthcare Group Eye Institute, Tan Tock Seng Hospital, Singapore, Republic of Singapore.

[23] University of Oxford, Oxford, United Kingdom.

[24] Wilmer Ophthalmological Institute, Johns Hopkins Hospital, Baltimore, Maryland.

[25] Doheny Eye Institute, David Geffen School of Medicine, University of California, Los Angeles, Los Angeles, California.

Financial Disclosure(s):
The author(s) have made the following disclosure(s): R.H.G.: Financial support — Novartis, Bayer, Apellis, Roche/Genentech.

P.J.R.: Financial support — Carl Zeiss Meditec, Genentech, Tyrogenex, Achillion Pharmaceuticals, Boehringer-Ingelheim, Carl Zeiss Meditec, Chengdu Kanghong Biotech, Healios K.K., Hemera Biosciences, F. Hoffmann-La Roche Ltd., Isarna Pharmaceuticals, Lin Bioscience, NGM Biopharmaceuticals, Ocunexus Therapeutics, Ocudyne, Unity Biotechnology; Equity owner — Apellis, Verana Health, Ocudyne.

C.A.C.: Financial support — Hoffman-LaRoche, Heidelberg Engineering.

F.G.H.: Financial support — Heidelberg Engineering, Optos, Zeiss, Novartis, Bayer Healthcare, Genentech, Acucela, Boehringer Ingelheim, Alcon, Allergan.

G.S.: Financial support — Heidelberg Engineering, Zeiss Meditec, Optovue, Optos, Centervue, Nidek, Novartis, Bayer; Non-financial support — Boeheringer, Allergan, Alcon.

K.B.F.: Financial support — Genentech/Roche, Heidelberg Engineering, Optovue, Allergan, Novartis, Carl Zeiss Meditec.

S.S.-V.: Financial support — Acucela, Alcon/Novartis, Allergan, Bayer, Bioeq/Formycon, Carl Zeiss MediTec AG, Centervue, Galimedix, Heidelberg Engineering, Katairo; Nonfinancial support — Optos.

J.S.: Financial support — Heidelberg Engineering, Alcon, Alimera, Janssen Research and Development LLC, Baxter Healthcare Corporation, Othera Pharmaceuticals, Inc., Bayer Healthcare, Pfizer, Astellas.

R.F.S.: Consultant — Topcon Medical Systems, Heidelberg Engineering; Royalties — Topcon Medical Systems, DORC.

A.T.: Financial support — Novartis, Roche, Bayer Healthcare, Allergan, Alcon, Heidelberg Engineering, Kanghong.

U.C.: Financial support — Novartis, Bayer, Allergan, Heidelberg Engineering.

G.J.J.: Financial support — Heidelberg Engineering.

K.C.: Financial support — Genentech, Regeneron, Heidelberg Engineering, Gyroscope, Roche, Allergan, Ophthotech, Acucela; Equity owner — Apellis.

D.S.: Financial support — Genentech, Heidelberg, Regeneron, Optovue, Topcon, Bayer, Novartis, Optovue.

J.M.M.: Consultant — Novartis, Bayer, Alcon, Roche, Genentech, Cellcure, Reneuron; Financial support — Eyerisk Consortium 2020, Novartis, Bayer, Alcon, Roche, Ophthotech; Equity owner — Ophthotech, Notalvision.

R.T.: Financial support — Novartis, Bayer, Allergan, Roche-Genetech, Thea, Alcon, Oculis.

F.B.: Financial support — Novartis, Bayer; Nonfinancial support — Allergan, Heidelberg Engineering.

S.L.: Financial support — Heidelberg Engineering, Carl Zeiss Meditec, Novartis, Allergan, Bayer; Nonfinancial support — Heidelberg Engineering, Carl Zeiss Meditec.

D.P.: Financial support — Roche, Novartis, Bayer; Consultant — Novartis, Bayer.

S.P.: Financial and Nonfinancial support — Novartis, Bayer, Allergan, Alcon, Heidelberg Engineering, Zeiss.

M.F.: Financial support — Heidelberg Engineering, Zeiss Meditech, Optos, Novartis, Bayer, Genentech, Roche; Nonfinancial support: Heidelberg Engineering, Zeiss Meditech, Optos; Patent - US20140303013 A1 pending.

T.H.L.: Nonfinancial support — Novartis, Heidelberg Engineering.

V.C.: Financial support — Boehringer Ingelheim International GmbH.

S.R.S.: Financial support — Optos, Carl Zeiss Meditec, Allergan, Carl Zeiss Meditec, Alcon, Allergan, Genentech, Regeneron, Novartis.

A list of Classification of Atrophy Meeting participants is available at www.aaojournal.org.

Acquisition of human donor eyes and the Project MACULA website were supported by the National Institutes of Health, Bethesda, Maryland (grant nos.: R01EY06019 [C.A.C.] and P30 EY003039 [C.A.C.]), the National Institutes of Health (grant nos.: R01EY024091 [J.S.], R01EY12951 [J.S.], R24 EY027285 [J.S.], and P30EY019007 [J.S.]); EyeSight Foundation of Alabama (C.A.C.); International Retinal Research Foundation (C.A.C.); the Edward N. and Della L. Thome Foundation (C.A.C.; J.S.); the Arnold and Mabel Beckman Initiative for Macular Research (C.A.C.; J.S.); Research to Prevent Blindness, Inc, New York, New York (C.A.C., J.S.); the Lowy Research Medical Institute (A.C.B.); the National Health & Medical Research Council of Australia (fellowship no.: GNT1103013 [R.H.G.]); Foundation Fighting Blindness (J.S.); and the National Institute for Health Research Biomedical Research Centre Moorfields Eye Hospital, London, United Kingdom (A.T.). Clinicopathologic correlation supported by the Macula Foundation, New York (C.A.C.).

HUMAN SUBJECTS: Human subjects were not included in this study. This was a consensus paper with no direct participants involved in this consenses.

No animal subjects were included in this study.

Author Contributions:

Conception and design: Guymer, Rosenfeld, Curcio, Holz, Staurenghi, Schmitz-Valckenberg

Analysis and interpretation: Guymer, Rosenfeld, Curcio, Holz, Staurenghi, Freund, Schmitz-Valckenberg, Sparrow, Spaide, Tufail, Chakravarthy, Jaffe, Csaky, Sarraf, Monés, Tadayoni, Grunwald, Bottoni, Liakopoulos, Pauleikhoff, Pagliarini, Chew, Viola, Fleckenstein, Blodi, Lim, Chong, Lutty, Bird, Sadda

Data collection: Guymer, Rosenfeld, Curcio, Holz, Staurenghi, Schmitz-Valckenberg, Sparrow, Spaide, Tufail, Chakravarthy, Jaffe, Csaky, Monés, Tadayoni, Grunwald, Bottoni, Liakopoulos, Pauleikhoff, Pagliarini, Viola, Fleckenstein, Blodi, Lim, Chong, Lutty, Bird

Obtained funding: Guymer, Rosenfeld, Curcio, Holz, Staurenghi, Freund, Schmitz-Valckenberg, Sparrow, Spaide, Tufail, Chakravarthy, Jaffe, Csaky, Sarraf, Monés, Tadayoni, Bottoni, Liakopoulos, Pauleikhoff, Pagliarini, Fleckenstein, Lim, Chong, Sadda

Overall responsibility: Guymer, Rosenfeld, Curcio, Holz, Staurenghi, Freund, Schmitz-Valckenberg, Sparrow, Spaide, Tufail, Chakravarthy, Jaffe, Csaky, Sarraf, Monés, Tadayoni, Grunwald, Bottoni, Liakopoulos, Pauleikhoff, Pagliarini, Chew, Viola, Fleckenstein, Blodi, Lim, Chong, Lutty, Bird, Sadda

Abbreviations and Acronyms:
AMD = age-related macular degeneration; **CAM** = Classification of Atrophy Meeting; **CFP** = color fundus photography; **cRORA** = complete retinal pigment epithelium and outer retinal atrophy; **ELM** = external limiting membrane; **EZ** = ellipsoid zone; **FAF** = fundus autofluorescence; **GA** = geographic atrophy; **GCL** = ganglion cell layer; **HFL** = Henle fiber layer; **INL** = inner nuclear layer; **IPL** = inner plexiform layer; **iRORA** = incomplete retinal pigment epithelium and outer retinal atrophy; **IZ** = interdigitation zone; **NFL** = nerve fiber layer; **nGA** = nascent geographic atrophy; **ONL** = outer nuclear layer; **OPL** = outer plexiform layer; **RPD** = reticular pseudodrusen; **RPE** = retinal pigment epithelium.

Correspondence:
Robyn H. Guymer, MBBS, PhD, Centre for Eye Research Australia, Level 7, 32 Gisborne Street, East Melbourne, Victoria 3002, Australia. E-mail: rhg@unimelb.edu.au.

Appendix 1.

List of CAM meeting participants (at least one meeting attended and consensus exercises completed):

Giovanni Staurenghi, Frank Holz, Daniel Pauleikhoff, Srinivas Sadda, Rick Spaide, Rick Ferris, Ferdinando Bottoni, Usha Chakravarthy, Emily Chew, Victor Chong, Karl Csaky, Christine Curcio, Ronald Danis, Francois Delori, Scott Fraser, K. Bailey Freund, Juan Grunwald, Robyn Guymer, Tock Han Lim, Jerry Lutty, Glenn Jaffe, Ivana Kim, Jordi Mones, Richard Rosen, Philip Rosenfeld, David Sarraf, Steffen Schmitz-Valckenberg, Sandra Liakopoulos, Janet Sparrow, Ramin Tadayoni, Francesco Viola, Akio Oishi, Sergio Pagliarini, Alan Bird, Barbara Blodi, Dean Bok, Petrus Chang, Gemmy Cheung, Stephano De Angelis, Andrew Dick, Deborah Ferrington, Jeff Fingler, Monika Fleckenstein, Andrea Giani, Carel Hoyng, Imre Lengyel, Andrew Lotery, Robert F. Mullins, Sobha Sivaprasad, Sebastian Wolf, and Ruikang Wang.